Characteristics of Summer Trade-Wind Rainfall over Oahu

Treena Marie Hartley[+] and Yi-Leng Chen[*]

Department of Meteorology

University of Hawaii

Honolulu, HI 96822

Submitted to *Weather and Forecasting*

Revised May 6, 2010

[*]*Correspondence author address*: Dr. Yi-Leng Chen, Dept. of Meteorology, SOEST, University of Hawaii at Manoa, Honolulu, HI 96822

Email: yileng@hawaii.edu

[+]Current affiliation: National Weather Service Weather Forecast Office, Eureka, California

ABSTRACT

In this study, characteristics of summer trade-wind rainfall over Oahu are analyzed. In the early morning before sunrise, flow deceleration on the windward coastal area is the greatest when the island land surface is the coldest. Furthermore, relatively calm winds are found over Central Oahu between the Ko'olau Mountains and the Waianae Mountains, with weak westerly katabatic winds on the windward side of the Waianae Mountains. Most windward stations have an early morning rainfall maximum with a secondary rainfall maximum in the early evening. Morning (afternoon) land (sea) breezes dominate under variable winds, and are more pronounced over leeward Oahu. Precipitation on the western leeside coast has a slight peak in the afternoon due to an increase of cloud development from the afternoon sea breezes.

Daily orographic rainfall over Oahu is greater under the strong trade-wind regime, and less under weak trade-wind and variable-wind flow regimes. However, the maximum correlation between daily trade-wind rainfall and trade-wind speed is < 0.3. Days with high rainfall generally occur under strong trades, but not all strong trade-wind days produce significant rainfall. With its relatively low terrain height compared to LCL (Lifted Condensation Level) and relatively small size, orographic lifting alone is inadequate to initiate precipitation through warm rain processes. The existence of trade-wind cumuli upstream is necessary. In addition, a deeper moist layer and higher moisture content upstream are two conditions that are favorable for higher orographic precipitation over Oahu under undisturbed summertime trade-wind weather.

1. Introduction

Under summer trade-wind conditions, there are large spatial variations of island-scale weather. The Hawaiian Islands are comprised of many microclimates such that the landscape of a particular island can change from desert like conditions to tropical rain forest over a short distance. Differences in the size, shape, position, and topography of each island in the Hawaiian Island chain contribute to the varying characteristics of island weather. The grid spacing of the Global Forecast System (GFS) is relatively large and does not depict island-scale weather with much precision. An improved understanding of island-scale weather over the Hawaiian Islands will benefit weather forecasts for Hawaii and other subtropical islands.

Leopold (1949) studied cloud patterns over the Hawaiian Islands resulting from local sea (land) breeze and mountain (valley) breeze interactions. Blumenstock and Price (1967) classified seven climatic regions for Hawaii: the windward lowlands (< 2000 ft on the north-northeast side of islands), the leeward lowlands, the interior lowlands (on Oahu and Maui), the Kona coast of Hawaii, the rainy mountain slopes on the windward side, the lower mountain slopes on the leeward side, and the high mountains. Lyons (1982) showed that trade wind induced rainfall is the dominant spatial and temporal Hawaiian rainfall pattern, and has a 90% frequency in summer compared to a 50% frequency in the winter. Giambelluca et al. (1986) suggest that orographic uplift, thermally driven wind, convection, and the position of the trade-wind inversion relative to the terrain contribute to the spatial distribution of rainfall over the Hawaiian Islands. Larson (1978) tracked trade-wind clouds from satellite data during the summer of 1976 and 1977 over the Hawaiian Islands and found that the advection of trade-wind clouds inland could account for heavy local showers. Ramage and Schroeder (1999) showed that the significant trade wind rainfall atop Mount Waialeale (1598 m MSL), Kauai is a result of moderate to fresh trade winds being lifted up the eastern escarpment of Waialeale, but only when a band or area of cumulus extends upwind of the mountain.

Island-scale weather and airflow have been studied extensively for the island of Hawaii [Project Shower (1954), Warm Rain Project (1965), Project Ahupua (1978), Hawaii Meso-scale Energy and Climate Project (1981), Joint Hawaiian Warm Rain Project (1985), and Hawaiian Rainband Project (1990)], which is the largest island of the Hawaiian Island chain. Two of the five volcanoes (Mauna Kea and Mauna Loa) that form the island stand above 4,000 m high; well above the typical height of the trade-wind inversion (TWI) (~2,000 m). Along the windward side, the orographically induced pressure gradient force slows and deflects the incoming trade-wind flow as a result of a low Froude-number (Fr = U/Nh, where U is the upstream wind speed, N is Brunt-Vaisala frequency, and h is the height of the barrier) flow regime past a 3-D barrier (Smolarkeiwicz et al. 1988). In addition to Fr, for mountains with tops well above the TWI, the TWI serves as a lid forcing the low-level flow to move around the terrain (Leopold 1949; Schär and Smith 1993) with maximum rainfall on the windward slopes (Giambelluca et al. 1986). Chen and Feng (2001) show that the TWI height represents the depth of the moist layer that affects cloud development and convective feedback to the island airflow (Chen and Feng 2001). Island surface winds also vary diurnally due to land surface heating (cooling) in the afternoon (morning) (Chen and Nash 1994; Chen and Feng 1998; Feng and Chen 2001). The land surface heating/cooling is sensitive to ground cover, soil properties and distributions of clouds and rain (Chen and Wang 1994; Zhang et al. 2005a). Daytime sea-breeze/upslope flow and nocturnal land-breeze/downslope flow often develop in weak wind regions and are more pronounced when the prevailing wind flow is light (Chen and Nash 1994).

Using HaRP (Hawaiian Rainband Project) data, Chen and Feng (1995) found that the daily rainfall on the windward side of the island of Hawaii is highly correlated with the 0200 HST TWI height at Hilo, with a maximum correlation greater than 0.7 at the windward coast. In addition to the TWI, the daily rainfall amount on the windward side is also affected by the upstream trade-wind speed (Esteban and Chen 2008). Except in the afternoon hours, rainfall amounts on the windward side are higher when trades are stronger. For weak trades, the rainfall distributions have a pronounced late afternoon maximum on the windward slopes due to the development of anabatic winds. Along the lee-side Kona coast, the rainfall is not correlated with the TWI height at Hilo (Chen and Feng 1995). Yang et al. (2008) showed that the Kona leeside has an evening rainfall maximum due to the convergence between the katabatic flow and the westerly reversed flow offshore, which is stronger and deeper with a higher moisture content when trades are stronger. Therefore, evening rainfall along the Kona coast is higher when trades are stronger.

Oahu is the most populated island of the Hawaiian chain, with more than 80% of the state population. Nevertheless, not much research on island-scale weather over Oahu has been documented. In contrast to the island of Hawaii, the mountains over Oahu are well below the TWI (~ 2,000 m). The terrain of Oahu consists of two parallel mountain ranges (Ko'olau and Waianae) almost perpendicular to the persistent trade winds (Fig. 1). The Ko'olau Mountain peaks range from approximately 500 to 960 m high, and extend about 45 km along Oahu's eastern coast. The Waianae Mountains range from 470 to 1,200 m high, and extend about 30 km along the western coast of Oahu. Nguyen et al. (2010) showed that under summer trade-wind conditions, $U/N > h$, low-level air parcels are able to ascend to the mountain tops of the Ko'olau Mountains throughout the diurnal cycle with mountain waves above the peak. In addition to having much lower terrain heights, Oahu's size is much smaller than the island of Hawaii. A recent modeling study by Yang and Chen (2008) suggests that mountains with peaks below the TWI height, on a relatively small island, have maximum rainfall at the mountain peaks.

Leopold (1948) noted the nocturnal wind speed minimum throughout the island of Oahu. The wind speed is stronger over the island interior in the afternoon due to vertical mixing of momentum caused by solar heating (Loveridge 1924). Leopold (1948) found that when the wind speeds are low, afternoon sea breezes occurred at all southern and Waianae stations of Oahu. From the analysis of rainfall data at 6 stations on Oahu, Leopold (1948) concluded that the rainfall from four Ko'olau stations is mainly from trade-wind orographic showers, whereas the rainfall for a Waianae station is from afternoon convective showers. Schroeder (1977) computed rainfall frequency from 38 stations for Oahu from March 1965 to December 1973 and found that the diurnal rainfall frequency amplitudes are relatively small at all stations except Lualualei (lee of the Waianae Mountains) which displayed an early morning rainfall maximum. Loveridge (1924) postulated that the observed nocturnal (1200 to 0800 HST) peaks in rainfall frequency (i.e. percentage of days with rainfall during the period) and rainfall accumulation at Honolulu were caused by nocturnal cloud-top radiative cooling.

Lavoie (1974) applied a simple mesoscale model to study the precipitation distributions for weak (~ 5 m s^{-1}), normal (7 m s^{-1}), and strong (11 m s^{-1}) summer trades during the daytime over Oahu. Under normal trades, the simulated rainfall rate was the greatest over the Ko'olaus (~ 1.5 mm day^{-1}), and much less over the Waianae Mountains (~ 0.5 mm day^{-1}). Under weak winds, the simulated rainfall was reduced over the Ko'olaus, and enhanced over the Waianae Mountains. Under strong winds, the simulated rainfall doubled over the Ko'olaus and there was no rainfall over the Waianae Mountains. Lavoie also showed that the simulated rainfall for the normal TWI height was the greatest over the Ko'olaus (~ 1.5 mm day^{-1}), and much less over the Waianae Mountains (~ 0.5 mm day^{-1}). No rainfall was simulated with a lower TWI.

With the deployment of the NWS hydronet rain gauges, there are currently 68 hourly rainfall stations over Oahu, including 39 stations with 0.01-inch resolution. There are also 13 wind measuring stations across Oahu. In this study, we used the dense surface data to study the airflow and rainfall distributions for the island of Oahu under summer trade-wind conditions. The diurnal variations of island-scale precipitation and wind during the summer months (May - July 2002 and May - September 2003) under different trade-wind conditions for Oahu were analyzed. Previous studies (e.g., Schroeder 1977) show that the diurnal rainfall signals over Oahu are small. However, these studies include rainfall data throughout the year including the winter storm season as well as days with synoptic disturbances during the warm season (May-October). A recent modeling study by Nguyen et al. (2010) suggests that despite its relatively small area (1,536 sq km), the island of Oahu has profound influences on airflow and weather throughout the diurnal cycle. In the present study, only undisturbed trade-wind days during the warm season were used to study how the summer trade-wind rainfall over Oahu is related to upstream trade-wind conditions (trade-wind speed, TWI height, moisture content and stability). Finally, the implications for forecasting summer trade-wind orographic rainfall over Oahu will be discussed.

2. Data and analysis procedures

a. Rainfall data

The hourly precipitation observations were collected for stations throughout Oahu from a variety of sources including, NWS Hydronet, United States Geographic Survey (USGS), Remote Automated Weather Station (RAWS), Marine Weather Transmitter (MWT), Automated Remote

Collector (ARC), Automated Surface Observing System (ASOS), and National Climate Data Center (NCDC) stations. A disadvantage of obtaining data from these various sources is an inconsistency in rainfall resolution. There are five different rainfall resolutions in the dataset (0.01 in, 0.083 in, 0.10 in, 0.12 in, 0.188 in) (Fig. 1a). Of these resolutions, the 0.01-in is the best for studying diurnal variability, since very light rainfall is detected at these stations. The data with resolutions greater than 0.01-in were used cautiously. Heavy rainfall events from synoptic disturbances were removed from the data. To determine which days had rainfall derived from synoptic disturbances, days recording hourly rainfall greater than 6 mm were identified. The 500-hPa and 25-hPa maps for these days were examined to determine if synoptic disturbances were present. Days affected by nearby upper-level troughs or lows, tropical disturbances or surface lows were excluded from our data set. For each station, hourly rainfall frequency and hourly rainfall rate were calculated for undisturbed trade-wind days. Hourly rainfall frequency was computed as the number of days with measurable rainfall in each hour divided by the number of days with observations for that hour. It is expressed as a percent. Hourly rainfall rate is defined as the total rainfall in each hour divided by the number of observations for that hour. Rainfall rate may be strongly affected by heavy trade-wind showers that occur at a specific location at a specific time. However, such an event would only contribute a single rainfall occurrence with a small influence on the hourly rainfall frequency.

b. Surface wind data

The hourly wind data include 13 stations on Oahu (Fig. 1b) from ASOS, MWT, ARC, and RAWS observation sites. There are differences in tower height and average sampling rate for the different wind observation sites. The RAWS stations record wind measurements from 6 m above ground, whereas the winds from the other stations are measured at 10 m. The wind data are measured every second at all stations. The data are averaged over a 2-min period for the ASOS and ARC stations, a 1-min period for the MWT stations, and a 10-min period for the RAWS stations. A correction factor of 1.086 was applied to the RAWS (6-m) stations to convert the 6-m wind speeds to 10-m values (Bradshaw et al. 2003).

The sampling period (May – July 2002 and May – September 2003) was based on data availability. The Lihue soundings at 1200 UTC during this period were retrieved from the University of Wyoming Meteorology web site (www.uwyo.edu). These soundings were used to determine the trade-wind inversion height for each day. The 1200 UTC wind data from the National Centers for Environmental Prediction/National Center for Atmospheric Research (NCEP/NCAR) reanalysis data for an upstream point (22.5^0N, 157.5^0W) are used to represent open ocean trade-wind conditions.

c. WSR-88D data

The WSR-88D Level-III 3-hr precipitation data (Fulton et al. 1998) from the Molokai radar (21.132^0N, 157.179^0W) is used to construct Oahu rainfall for July-August 2005. The radar data provide rainfall information over the ocean upstream in comparison to rainfall over land.

d. Analysis procedures

To test if the chosen time period is representative of climatology, monthly rainfall accumulation was compared with the monthly climatologic normal rainfall for 28 Oahu stations. The monthly rainfall and normal values were obtained from the NWS Monthly Precipitation Summaries, and the normal values are based on 30 years of data (1971-2000). The monthly rainfall accumulation and normals were added for all months within the period of study. The percentage of rainfall from the norm was determined by dividing the rainfall accumulation by the 'normal' rainfall (Table 1). Most stations (20/28) had less than normal rainfall (< 90%). A few stations (4/28) had rainfall no more than 10% higher of the norm, and 4 stations had rainfall slightly greater than 110%.

A histogram of the daily upstream 1200 UTC wind direction for all days during the period of study (2002 May – July and 2003 May – September) was constructed using the NCEP/NCAR reanalysis data at 22.5^{0}N, 157.5^{0}W. Most of the daily wind was northeasterly (0^0 to 90^0) with a peak daily wind direction occurrence at 90 degrees (not shown). Two main wind categories were defined from these data; variable winds and east-northeast (ENE) trade winds. Variable winds were defined as wind (from any direction) with speed < 3 m s^{-1}. ENE trade winds were defined as wind between 70^0 and 90^0 (with speed > 3 m s^{-1}). The ENE trade winds were further divided into three groups based on wind speed [strong trade winds, normal trade winds, and weak trade winds] (Table 2).

Since the focus of this study is on island-induced weather under normal trade-wind conditions, rainfall events from synoptic disturbances were removed from the sample. Synoptic charts at 500-hPa and 250-hPa levels for these days were examined to determine if synoptic disturbances were present. Days with nearby upper or mid-level troughs or lows, tropical disturbances, or unseasonable surface lows were defined as days influenced by synoptic conditions (6, 15 May, 2002 and 4-8 June, 24-27 July, 10-11 September, 2003).

Three TWI height categories (Low, Normal, and High) were defined based on the histogram of daily TWI heights for all days during the period of study (not shown). Low TWI days were defined as days having a base less than 1,675 m, normal TWI days were between 1,676 and 2,319 m, and high TWI days > 2,320 m (Table 3). The trade-wind inversion height was always above the Oahu mountains during the study period. The mean and standard deviations for each TWI category are listed in Table 3. The correlation between TWI height and daily trade-wind rainfall for each station was computed. Scatter plots (with regression line and correlation values) for TWI height and daily rainfall accumulation for all stations with 0.01-in rainfall resolution were also constructed.

Three moisture categories (Low, Normal and High) were also defined based on the 925-hPa relative humidity (RH) at an upstream point (22.5^{0}N, 157.5^{0}W) (Table 4). Three stability categories (Low, Normal, and High) were defined based on the differences in the potential temperature between 925 hPa and 850 hPa at the same upstream point (Table 5).

3. Diurnal variations of surface winds

The mean hourly atmospheric temperature over the Honolulu International Airport [HNL -Station 1 (Fig. 1)] during the period of study ranged from 24.2^{0}C to 30.0^{0}C, with an afternoon (1400 HST) maximum. The diurnal variations in surface air temperature over land would result in diurnal driven flow (Nguyen and Chen 2010) especially under weak and variable wind conditions.

a. ENE Trades

Along the windward coast, winds are weaker than the upstream values for both the strong and weak trade-wind regimes, especially in the early morning when the land surface is the coldest (Fig. 2). The deceleration of the trade winds on the windward side in the early morning is more significant when trades are stronger (4-7 m s^{-1} at the coast vs. 8-10 m s^{-1} over the open ocean) as a result of orographic blocking. In the afternoon, winds along the windward coast are stronger than any other time of the day as a result of combined onshore/trade-wind flow. Over Central Oahu, winds are relatively calm (~ 1 m s^{-1}) in the early morning, with westerly katabatic flow on the windward side of the Waianae Mountains, and shift to easterly trades (2-4 m s^{-1}) after sunrise (Fig. 2). For most stations over the island interior, the easterly winds are 2-3 m s^{-1}

stronger in the afternoon than in the morning due to vertical mixing of momentum as a result of daytime heating (Fig. 2) (Zhang et al. 2005b). Along the south shore, winds are stronger in the afternoon compared to the early morning (5-7 m s^{-1} vs. 2-4 m s^{-1}) during strong trades. For weak trades, winds exhibit an offshore flow component in the early morning. Along the leeward coast, afternoon sea-breezes are observed under weak trades (Fig. 3).

b. Variable winds

Stations on the windward side (Station 3, 4, 5, 8, Fig. 1b) do not show wind shift throughout the diurnal cycle (Fig. 3a). However, with nighttime cooling, winds are relatively weak at night (Fig. 3b). During the daytime, winds are stronger than the upstream values (< 3 m s^{-1}), as the incoming weak trade-wind flow is enhanced by upslope/onshore flow as a result of solar heating. Stations along the windward coast have stronger easterly winds in the afternoon than the rest of the day for the variable-wind flow regime (Fig. 3b).

Locally driven diurnal winds are significant under the variable wind regime, especially over the island interior and on the lee side. Land (sea) breezes dominate the western lee side and the south shore of Oahu (Fig. 3a) (Station 1, 2, 9, 10, 11, Fig. 2). The daytime sea breezes and nighttime land breezes along the south shore (Station 1, 2) extend farther inland reaching central Oahu (Station 7 and 13) (Fig. 3a) with wind speeds less than 2 m s^{-1} (Fig. 3b). The diurnal winds along the northern Waianae lee-side coast are also light (< 2-3 m s^{-1}). Station 12 on the windward foothills of the Waianae Mountains shows nighttime westerly katabatic flow.

4. Diurnal variations of hourly rainfall frequency

In this section, time series plots of diurnal rainfall frequencies for stations with 0.01-in resolution will be used to study the diurnal variations of rainfall. As will be shown later, most stations east of the Waianae Mountain Range have an early morning (0600 - 0800 HST) rainfall frequency maximum. Some of these stations with a morning or nocturnal rainfall frequency maximum have a secondary maximum in the early evening. Furthermore, most stations near the Waianae Mountain Range have a small afternoon rainfall frequency maximum**.**

a. ENE Trades

Most stations over the windward side and the Ko'olau Mountains with 0.01-in resolution exhibit an early morning maximum for ENE trade-wind days (Figs. 4a, b). Over the windward foothills, an early morning hourly rainfall maximum, with secondary evening rainfall maximum, is observed (Fig. 4a). In addition to cloud top radiative cooling (Loveridge 1924; Schroeder 1977), convergence due to the early morning airflow deceleration offshore and lower LFC (level of free convection) at night would explain the morning rainfall maximum along the windward foothills and over the Ko'olau Mountains (Nguyen et al, 2010). A secondary evening rainfall maximum (~15-25% frequency) occurs near 1900 HST (Fig. 4a). The evening rainfall maximum may be related to enhanced orographic lifting after sunset by stronger winds above due to less mixing of momentum as the land surface cools (Nguyen et al. 2010).

Over Central Oahu in the lees of the Ko'olau Mountains, with the absence of orographic lifting, nocturnal rainfall is less frequent than at stations over the Ko'olau Mountains (Fig. 4d). In the early morning and at night, the remnants of orographic clouds from the Ko'olau Mountains drift over Central Oahu, especially under stronger trade-wind conditions. Except along the Waianae coast, most stations exhibit an afternoon minimum in hourly rainfall occurrences (Figs. 4a, b and c). This diurnal rainfall minimum is related to vertical mixing over land with a relatively higher LFC (~ 900 m at 2 pm vs. 700 m at night), as the drier air aloft mixes with relatively moist air in low levels (Nguyen et al. 2010).

Over Waianae, a small afternoon maximum rainfall frequency is evident (Fig. 4b). Trade-wind rainfall is infrequent in this area with a small early afternoon maximum (5%) (Fig. 4b). Trade-wind cumuli moving over the Ko'olau Mountains release some of the condensates there, and thus, the air moving over the Waianae Mountains is relatively dry. The small afternoon maximum in hourly rainfall frequency is mainly due to the increase in afternoon cloudiness in response to the development of sea breezes, especially under weak wind conditions.

b. Effects of trade-wind speed on rainfall occurrences

The diurnal variations of hourly rainfall frequency for days with normal trades (not shown) are very similar to those for all ENE trade-wind days (Fig. 4). For strong trade-wind days, trade-wind showers are more frequent (Fig. 5) than for all ENE trade-wind days, for most stations (Fig. 4) throughout the diurnal cycle. The twice daily rainfall frequency maxima for windward foothill stations are more significant for strong trade-wind days (25-40% near 0700 HST and 20-30% at 1900 HST) (Fig. 5a) than for weak trade-wind days (Fig. 6a). For strong trade-wind days, most Ko'olau Mountain stations have frequent (25-50%) nocturnal (2100-2300 HST) and early morning (0700-0900 HST) (15-40%) trade-wind showers (Fig. 5c). For weak trade-wind days, the hourly rainfall frequencies for the Ko'olau stations are a lot lower throughout the diurnal cycle (Fig. 6c) than for strong trade-wind days. Thus, the nocturnal/early-morning rainfall maxima over the Ko'olau Mountains may not be simply caused by cloud top radiative cooling. The decrease in trade-wind speed at night and in the early morning as the trade-wind flow approaches the cooler island land mass is also important. The decrease in wind speed on the windward side is greater under strong trades than under weak trades (Fig. 2).

For strong trade-wind days, Central Oahu has a morning (near 0500 HST) rainfall frequency maximum (~ 10%), and a secondary nocturnal (near 2200 HST) maximum (~ 10%)

(Fig. 5d). For weak trade-wind days, rainfall over Central Oahu is infrequent (Fig. 6d). Of all ENE trade-wind days, the afternoon rainfall minimum over the Ko'olau Mountains and Central Oahu is most pronounced under the strong trade-wind regime (Figs. 4, 5, and 6). It is expected that the vertical mixing in the afternoon over land is more significant when trades are stronger (Zhang et al. 2005b) and there is a higher LFC.

The diurnal variations of rainfall frequency for Waianae are rather small for both strong and weak trade-wind days (Figs. 5b and 6b). Hourly rainfall frequencies are higher for strong trades than weak trades, in contrast to the results from the previous modeling study by Lavoie (1974) who predicted no rainfall over the Waianae Mountains under strong trades. Station 59 is at a higher elevation (1,750 ft) than the other stations in the area. It records slightly higher hourly rainfall frequencies than other stations, especially when the trade winds are stronger (Fig. 5b).

5. Relationship between daily trade-wind rainfall and trade-wind speed

The daily trade-wind rainfall is the largest (2-6 mm) over the Ko'olau Mountains compared with other areas over Oahu (Fig. 7). The daily trade-wind rainfall over Central Oahu is much less (< 1 mm) than over the Ko'olau Mountains and the windward foothills. A secondary maximum in daily rainfall (> 1 mm) occurs over the Waianae Mountains. The leeward coastal areas receive the least amount of rainfall.

When the trade winds are stronger, the daily rainfall amount is higher (Fig. 7). The orographic lifting would be greater for stronger trades, thus creating higher rainfall amounts (6-10 mm) over the Ko'olau Mountains than weak trades (1-4 mm). Central Oahu has approximately 1 to 2 mm of daily rainfall under strong trades as compared to < 1 mm for weak trades. The daily maximum rainfall amount over the high peaks of the Waianae Mountains is greater than 2 mm for strong trades as compared to < 1 mm for weak trades (Fig. 7). Most of the island receives less than 1 mm of rainfall when the winds are variable, and only the northern Ko'olau Mountain range receives daily rainfall >1 mm during these periods (Fig. 7d).

The daily rainfall decreases for trade-wind regimes at lower speeds (Fig. 7). However, the correlation values between daily rainfall accumulation and trade-wind speed computed for all days with ENE trades (Fig. 8) are relatively small with maximum correlations slightly greater than 0.3 located over the highest elevations of the Ko'olau Mountains and the Waianae Mountains (Fig. 8). The correlations over the remainder of the Ko'olau and Waianae Mountains are slightly greater than 0.2. The relatively small correlations suggest that trade-wind intensity is not the only factor controlling Oahu rainfall production. Days with more rainfall tend to occur when trade winds are stronger, but days with strong trade winds do not necessarily have high rainfall amounts (Fig. 8). In the lee sides of both the Ko'olau and Waianae Mountains, the correlation is slightly negative due to stronger descending airflow under stronger trades.

Several previous authors have suggested the importance of upstream cloudiness on the production of local orographic showers (Mordy and Eber 1954; Siler 1962; Woodcock 1975; Larson 1978). Woodcock (1975) shows that the continuous orographic showers over the Ko'olau Mountains on 24 March 1965 were from a pre-existing layer of warm stratocumulus causing raindrop-generating processes to occur over the island. Orographic lifting alone may not have been adequate to explain this amount of rainfall as the events time frame was insufficient for raindrop formation to occur (15-20 minutes are required for air parcels from the shore to reach the mountain tops). Ramage and Schroeder (1999) studied trade-wind rainfall atop Mount Waialeale, Kauai (1,598 m MSL) between 1 May and 31 December for a relatively dry year (1976) and wet year (1982). They found the correlation between the trade-wind rainfall atop Mount Waialeale and trade-wind strength measured by rawinsondes at Lihue to be 0.34 and 0.31

for year 1976 and year 1982, respectively. Ramage and Schroeder noted that "although > 50 mm fell on 26 days of fresh trade winds, < 6 mm fell on other fresh trade wind days". They suggested that, "Cloudiness is the differentiator". Except for Larson (1978), the studies cited above include cases where synoptic disturbances were present. The pre-existing stratocumulus cloud deck studied by Woodcock (1975) was in the post-frontal area of a mid-latitude cold front.

Without the influences of synoptic/mesoscale disturbances, trade-wind showers during the summer months are intermittent, falling from trade-wind cumuli with relatively small sizes (< 5 km) as they drift inland (Larson 1978). Even though orographic showers are frequent over the Ko'olau Mountains, they do not occur every day. Even under persistent lifting by strong trades, the probability of trade-wind showers to occur over the ridge tops for any specific day is only about 80% (not shown). It is interesting to note that the LCL (Lifted Condensation Level) for typical trade-wind conditions is about 400 m at night and close to 800 m in the early afternoon (Nguyen et al., 2010) and is comparable or slightly lower than the ridge tops (500-960 m). Thus, if condensation occurs before the air parcel reaches the ridge tops due to orographic lifting, with its relatively small size, the advection time for the air parcel to reach the ridge tops after reaching the LCL is apparently too short (< 5-10 minutes) for the initiation of precipitation through the collision-coalescence process (~20 minutes) (Takahashi 1988). This fact clearly shows that pre-existing trade-wind cumuli are needed for the initiation of orographic rainfall over the Ko'olau Mountains. Figure 9 shows the summer trade-wind rainfall totals over Oahu for July-August 2005 measured by the surface network and the Molokai radar. Note that radar derived rainfall over the ridge tops could possibly be contaminated by ground clutter. Nevertheless, it is striking that on the windward side of the northeastern arm of the Ko'olau Mountains (Fig. 9a), significant rainfall totals are not observed over the relatively flat northeastern coast before the trade-wind flow reaches the foothills. It is apparent that significant orographic precipitation over the southern arm of the mountains occurs inland. In contrast, over the northern part of the Ko'olau Mountains, with relatively steep terrain along the coast, significant rainfall (> 100 mm) was observed along the coast as compared to the ridge tops (> 500 mm) (Fig. 9a). Nevertheless, the radar observed rainfall diminishes rapidly offshore (Fig. 9b). It is apparent that orographic precipitation from trade-wind cumuli, for the northern part of the Ko'olau Mountains, frequently starts immediately offshore as they move toward the coast.

6. Relationship between daily trade-wind rainfall and TWI height

In this section, the relationship between TWI height and daily rainfall will be discussed. With a higher TWI height, trade-wind cumuli could grow taller. Under a normal TWI height, a high-pressure cell (1024 hPa) is northeast of the islands near 34ºN 148ºW (not shown). When the TWI is high, this pressure cell shifts northeastward to 36ºN 142ºW (Fig. 10a) and is slightly stronger (1026 hPa). During low TWI height days, the pressure ridge shifts southward and the surface pressure over the islands is about 1- 2 hPa higher than the high TWI days (Fig. 11b).

Under a normal TWI height, the daily rainfall is similar to normal trade-wind conditions (not shown). For high TWI days, the daily rainfall has a maximum axis (> 4 mm) over the ridge tops of the Ko'olau Mountains, with a local maximum > 8 mm (Fig. 11a). For most areas over Oahu, daily rainfall is greater for high inversion days than normal trade-wind days. During low TWI days, the daily maximum rainfall axis along the ridge axis of the Ko'olau Mountains is > 2 mm with the daily rainfall maximum (> 6 mm) over the southeastern arm (Fig. 11b). The daily rainfall frequencies over the Ko'olau Mountains are also slightly lower (Fig. 11d) as compared with the high TWI cases (Fig. 11c). Over the Waianae Mountains, the daily rainfall frequencies

(20% vs. 40%) and daily rainfall accumulation (< 1 mm vs. > 1 mm) are also lower for low TWI-height days than high TWI-height days.

The correlation values between daily TWI heights and Oahu daily rainfall accumulation over the Ko'olau Mountains are between 0.1 and 0.3 (Fig. 12). The correlation values are lower (~0.1) over the Waianae Mountain Range (Fig. 12). The correlation over the Ko'olau Mountains is a lot lower compared to the value of 0.7 found for the rainfall at Hilo on the windward side of the island of Hawaii (Chen and Feng 1995) and > 0.4 for the rainfall atop Mountain Waialeale, Kauai (Ramage and Schroeder 1999). It is worth noting that the linear correlation between trade-wind speed and TWI height is low (~ 0.1) (Fig. 13a), in agreement with Ramage and Schroeder.

7. Relationship between low-level moisture and daily trade-wind rainfall

The 925-hPa relative humidity (RH) from the 1200 UTC NCEP/NCAR reanalysis data at the upstream point (22.5^{0}N, 157.5W) is used as a parameter to describe the low-level moisture content for the large-scale environment (Table 4). With a higher RH, less orographic lifting is required before the low-level air becomes saturated. The RH and TWI are weakly correlated (~ 0.13) (Fig. 13b). The correlation between the RH and daily wind speed is also low (-0.1) (Fig. 13c). For high RH days, the subtropical high has a relatively large East-West extent (Fig. 14a). For low RH days, a weak mid-latitude trough is to the northeast of the Hawaiian Islands (not shown) with the center of the subtropical high shifted to the south of its normal position (Fig. 14b) allowing drier air from mid-latitudes to push southeastward.

With a lower moisture content, the daily rainfall amount over the Ko'olau Mountains is lower, with maxima < 6 mm, as compared to normal trade-wind conditions (> 6 mm) (Fig. 7a) and high RH days (Figs. 15a, b). Over the Waianae Mountains, the daily rainfall maximum is > 1 mm for high RH days but is much less than 1 mm for low RH days. The horizontal distribution of correlation between RH and daily rainfall (Fig. 16) is slightly greater than 0.1 over the windward side of the Ko'olau Mountains and slightly greater than 0.2 over the Waianae Mountains. Thus, except over the Waianae Mountains, the relationship between RH and daily rainfall is less significant as compared to trade-wind speed and TWI height. The orographic precipitation over the Ko'olau Mountains due to orographic lifting is less under low RH days, but a higher moisture content may not necessarily produce more rainfall. The Waianae Mountains is under a rainshadow effect by the Ko'olau Mountains. Relatively dry air impinges on the Waianae Mountains because of descending airflow in the lee of the Ko'olau Mountains, and the possible removal of moisture by orographic precipitation over the Ko'olau Mountains. Light orographic precipitation over the Waianae Mountains is likely when the upstream air over the open ocean contains sufficient moisture, and light orographic showers are more frequent (> 40%) for high RH days than for low (> 10%).

The possible relationship between thermodynamic stratification within the trade-wind layer and daily rainfall amount was also investigated by using the differences between the 925 hPa and 850 hPa potential temperatures at the upstream point (22.5^{0}N, 157.5^{0}W) as a measure of stability. The day-to-day differences in stability are rather small, ranging from -2 to -4 K (Table 5), with more than 50% of the days between -2.4 and -3.5 K. For both low stability and high stability days, the daily rainfall amounts over the Ko'olau Mountains are similar to normal trade-wind days (~ 6 mm) (not shown). With relatively small variations in day-to-day stability, there are few differences in daily rainfall among the three categories.

8. Summary

Despite Oahu's relatively small size, the surface airflow and rainfall over the island are strongly modulated by the diurnal heating cycle under summer trade-wind conditions. Along the windward coast, the wind speeds are lower than over the open ocean, especially in the early morning when the island land surface is the coldest. The deceleration of the trade winds along the windward coast is more significant when trades are stronger (4-7 m s^{-1} at the windward coast vs. 8-10 m s^{-1} over the open ocean) as a result of orographic blocking. For most areas over Oahu, except along the western leeside coast, trade-wind speeds are 2-3 m s^{-1} greater in the early afternoon than during the early morning due to downward transport of trade-wind momentum in the afternoon hours. Over Central Oahu, in the lee of the Ko'olau Mountains, winds are calm (~ 1 m s^{-1}) at night but exhibit easterly trades (2-4 m s^{-1}) in the early afternoon. On the windward foothills of the Waianae Mountains, weak (1 m s^{-1}) westerly katabatic flow is observed in the early morning with easterly trades of 3-4 m s^{-1} in the afternoon. Along the western lee-side Waianae coast, sea breezes develop in the afternoon hours under weak (4-6 m s^{-1}) trade-wind and variable wind (< 3 m s^{-1}) conditions.

The daily rainfall frequencies over Oahu are the largest on the windward slopes (> 80%) of the Ko'olau Mountains with the maximum rainfall accumulation axis (> 6 mm) over the ridge tops. Most windward stations, and over the Ko'olau Mountains, have an early morning rainfall maximum which is more significant on strong trade-wind days than on weak trade-wind days. It is postulated that in addition to cloud top radiative cooling, the nocturnal rainfall maxima in those areas is due to the combination of orographic lifting and nocturnal deceleration of the prevailing airflow. Stations at the foothills of the Ko'olau Mountains exhibit an early evening (1900 HST) maximum. The evening rainfall maximum may be related to stronger orographic lifting due to stronger trade winds aloft after sunset as the land surface cools. Trade-wind rainfall is infrequent over Central Oahu and mainly results from the drifting of trade-wind showers downstream from the Ko'olau Mountains, especially under strong trade-wind conditions. A relatively small (< 10%) afternoon maximum in hourly rainfall frequencies is evident along the western leeside coast in response to the development of afternoon sea breezes.

When forecasting summertime orographic rainfall over Oahu under undisturbed trade-wind conditions, wind speed, inversion height and moisture content are three parameters to be considered, especially the wind speed. With more significant uplift, daily orographic rainfall over the Ko'olau Mountains is higher during stronger trades. Nevertheless, the daily trade-wind orographic rainfall and trade-wind speed are weakly correlated (< 0.3). Days with high rainfall generally have strong trade winds, but not all days with strong trades produce significant rainfall. For a subtropical island of relatively small size with ridge tops comparable or slightly higher than the LCL, orographic lifting alone is inadequate for the initiation of precipitation. If condensation occurs before the air parcel reaches the ridge tops, the advection time for the air parcel to reach the ridge tops after reaching the LCL is apparently too short (< 5-10 minutes) for the initiation of precipitation through the collision-coalescence process (~20 minutes). Pre-existing trade-wind cumuli are needed for the initiation of orographic rainfall over the Ko'olau Mountains. Thus, the use of satellite and radar observations to monitor upstream cloudiness and trade-wind showers is imperative for short-term forecasts of summertime orographic precipitation over Oahu.

Daily rainfall is greater over most areas of Oahu for the high TWI category with a maximum daily rainfall axis > 8 mm over the ridge tops. Due to the deeper moist layer present under these conditions, trade-wind cumuli can grow taller when the TWI height is higher. However, not all higher trade-wind inversion days produce more orographic rainfall over the Ko’olau Mountains as the maximum correlation between the daily rainfall and trade-wind inversion height is only slightly greater than 0.2. The trade-wind orographic rainfall is also affected by the moisture content of the trade-wind flow but to a much lesser extent compared to trade-wind speed and TWI height. Orographic rainfall over the Ko'olau Mountains is slightly higher when RH is higher. The daily orographic trade-wind rainfall over the Ko'olau Mountains is not sensitive to stability within the trade-wind layer. The daily variations in stability, measured as the differences in potential temperature between 925 hPa and 850 hPa, are relatively small.

Acknowledgements

This work was supported by NOAA under Cooperative Agreement Number NA17RJ1230 and COMET/UCAR under partners project grant S06-58389. We would like to thank Hiep V. Nguyen, Chuan-Chi Tu and Chunhua Zhou for their assistance, David Hitzl for editing the text, and anonymous reviewers for their comments.

References

Blumenstock D.I., and S.P., Price, 1967: Climates of the States - Hawaii. Environmental Data Service NOAA, 27 pp.

Bradshaw L.S., et al., 2003: An initial analysis of relationships between 2- and 10-minute averaged winds at 10, 6, and 1.8 meters: Implications for fire behavior and danger applications. *5th Symposium on Fire and Forest Meteorology*, 16 – 20 November 2003. Orlando, Florida.

Chen, Y.-L., and J.-J. Wang, 1994: Diurnal variation of surface thermodynamic fields on the island of Hawaii. *Mon. Wea. Rev*., **122**, 2125-2138.

—, and J. Feng, 2001: Numerical simulations of airflow and cloud distributions over the windward side of the island of Hawaii. Part I: The effects of trade wind inversion. *Mon. Wea. Rev*., **129**, 1117-1134.

—, and —, 1995: The influence of inversion height on precipitation and airflow over the Island of Hawaii. *Mon. Wea. Rev.*, **123**, 1660-1676.

Esteban, M. A., and Y.-L. Chen 2008: The impact of trade wind strength on precipitation over the windward side of the Island of Hawaii. *Mon. Wea. Rev*., **136**, 913-928.

Feng, J., and Y.-L. Chen, 2001: Numerical simulations of airflow and cloud distributions over the windward side of Hawaii. Part II: Nocturnal flow regime. *Mon. Wea. Rev.*, **129**, 1135-1147.

—, and —, 1998: The evolution of katabatic flow on the island of Hawaii during 10 August 1990. *Mon. Wea. Rev.*, **126**, 2185-2199.

Fulton, R., J. Breidenbach, D.-J. Seo, D. Miller, and T. O'Bannon, 1998: The WSR-88D rainfall algorithm. *Wea. Forecasting,* **13,** 377–395.

Giambelluca, T.W., M.A., Nullet, and T. A., Schroeder, 1986: Rainfall Atlas of Hawaii. Dept. of Land and Natural Resources, Division of Water and Land Development, Honolulu, HI (Report No. R76).

Larson, R. N., 1978: Summer trade wind rainfall in the Hawaiian Islands. *M.S. thesis*, Univ. of Hawaii*,* 85 pp. [Available from Dept. of Meteorology, Univ. of Hawaii, 2525 Correa Rd. Hon, Hi. 96822.]

Lavoie, R.L., 1974: A Numerical Model of Trade Wind Weather on Oahu. *Mon. Wea. Rev.*, **102,** 630 –637.

Leopold, L. B., 1948: Diurnal Weather patterns on Oahu and Lanai, Hawaii. *Pacif. Sci*., **2**, 81-95.

—, 1949: The Interaction of Trade Wind and Sea Breeze, Hawaii. *J Meteor.*, **6,** 312 – 320.

Loveridge, E. H., 1924: Diurnal Variations of Precipitation at Honolulu, U.S. *Mon. Wea. Rev.*, **52**, 584-585.

Lyons, S. W., 1982: Empirical orthogonal function analysis of Hawaiian rainfall. *J. of Appl. Meteor.*, **21**, 1713-1729.

Mordy, W. A., and L. E. Eber: Observations of rainfall from warm clouds. *Quart. J. Roy. Meteor. Soc.*, **80,** 48-57.

Nguyen, H. V., Y.-L. Chen, and F. M, Fujioka, 2010: Numerical simulations of island effects on airflow and weather during the summer over the island of Oahu. *Mon. Wea. Rev.*, (In press).

Ramage, C.S., and T. A. Schroeder, 1999: Trade Wind Rainfall atop Mount Waialeale, Kauai. *Mon. Wea. Rev.* Vol. **127**.

Riehl, H. 1979: Climate and Weather in the Tropics. Academic Press, 611 pp.

Schroeder, T. A., B. Kilonsky, and B. Meisner, 1977: Diurnal Variation in Rainfall and Cloudiness. *Water Resources Research Center Technical Report No. 112.*

Siler, R. K., 1962: Synoptic patterns for wet and dry trades on the island of Hawaii. *Mon. Wea. Rev.*, **90**, 103-106.

Smolarkiewicz, P. K., R. M. Rasmussen, and T. L. Clark, 1988: On the Dynamics of Hawaiian Cloud Bands: Island Forcing. *J. Atmos. Sci.,* **45**, 1872 – 1905.

Takahashi, T., 1988: Long-lasting trade-wind showers in a three-dimensional model. *J. Atmos. Sci.*, **45**, 3333-3353.

Woodcock, A. H., 1975: Anomalous orographic rains of Hawaii. *Mon. Wea. Rev.*, **103**, 334-343.

Yang, Y., and Y.-L. Chen, 2008: Effects of terrain heights and sizes on island-scale circulations and rainfall for the island of Hawaii during HaRP. *Mon. Wea. Rev.*, **136**, 120-146.

—, —, and F. M. Fujioka, 2008: Effects of trade-wind strength and direction on the leeside circulations and rainfall of the island of Hawaii *Mon. Wea. Rev,* **136**, 4799–4818.

—, and —, 2003: Circulations and rainfall on the lee side of the island of Hawaii during HaRP. *Mon. Wea. Rev.*, **131**, 2525-2542.

Zhang, Y., Y-L Chen, T. Schroeder and K. Kodama, 2005a: Numerical simulations of sea-breeze circulations in northwest Hawaii. *Wea and Forecasting*, **20**, 827-846.

—, —, S.-Y. Hong, K. Kodama, and H.-M. H. Juang, 2005b: Validation of the coupled NCEP Mesoscale Spectral Model and an advanced Land Surface Model over the Hawaiian Islands. Part I: Summer trade-wind conditions over Oahu and a heavy rainfall event. *Wea. Forecasting*, **20**, 847-872.

List of Tables

Table 1. Rainfall percentage from the climate norm for select stations over Oahu (% Norm). The rainfall accumulation was added from May – July 2002 and May - September 2003.

Stations	Latitude	Longitude	Rainfall (mm)	Norm (mm)	%Norm
Ahuimanu	21.43	-157.85	99.64	118.36	84.18
Aloha Tower	21.3	-157.87	10.01	21.59	46.35
Hakipuu M	21.5	-157.85	83.11	81.53	101.93
Hawaii Kai GC	21.3	-157.67	14.55	17.27	84.26
HNL AP	21.3	-157.94	8.71	11.68	74.57
Kahuku	21.7	-157.99	47.83	45.21	105.79
Kamehame	21.32	-157.69	12.14	22.86	53.11
Kunia Substation	21.4	-158.03	14.73	18.54	79.48
Lualualei	21.42	-158.14	24.38	19.81	123.08
Luluku	21.39	-157.81	108.53	94.74	114.56
Manoa Lyon	21.33	-157.8	191.21	259.59	73.66
Maunawili	21.35	-157.77	80.57	92.96	86.67
Mililani	21.47	-158.0	55.85	30.23	122.77
Moanalua	21.37	-157.83	43.61	92.71	47.04
Niu Valley	21.3	-157.73	32.00	37.59	85.14
Nuuanu WS	21.35	-157.82	83.52	135.64	61.57
Olomana	21.38	-157.75	34.80	46.74	74.46
Palisades	21.43	-157.95	54.86	89.41	61.36
Palolo FS	21.3	-157.8	21.13	42.42	49.82
Poamoho	21.55	-158.1	50.70	45.97	110.28
Punaluu	21.58	-157.9	71.76	83.57	85.87
Waianae	21.45	-158.18	9.02	10.16	88.75
Waiawa	21.45	-157.97	45.39	55.89	81.23
Waihee Pump	21.45	-157.85	127.58	142.24	89.7
Waimanalo	21.33	-157.72	16.43	40.89	40.19
Waipio	21.42	-158.0	43.89	64.52	68.03
Wheeler	21.48	-158.05	46.48	45.72	101.67
Wilson Tunnel	21.38	-157.82	165.46	150.62	109.85

Table 2. Statistics for ENE trade-wind categories determined from the 1200 UTC NCEP/NCAR reanalysis data from an upstream point (22.5°N, 157.5°W).

Statistics for Defined Trade Days					
Wind	Wind Speed (m/s)		Direction (deg.)		Sample Size
Category	Mean	St. Dev	Mean	St. Dev	n
Strong	8.7	0.52	85.3	4.20	20
Normal	7.0	0.55	84.6	5.09	73
Weak	5.1	0.49	85.1	4.41	15
Variable	2.0	0.64	169.6	87.8	20

Table 3. Statistics for TWI categories. The TWI height was determined from the 1200 UTC sounding data at Lihue, Kauai from May-July 2002 and May- September 2003.

Statistics for Inversion Height Categories				
Category	**Heights (m)**	**Mean (m)**	**St. Dev. (m)**	**n**
Low	< 1675	1516	164	28
Normal	1676-2319	2015	179	55
High	>2320	2635	288	25

Table 4. Statistics for RH categories determined from the 1200 UTC NCEP/NCAR reanalysis data from an upstream point (22.5°N, 157.5°W).

Statistics for 925 mb Relative Humidity				
Category	**RH (%)**	**Mean (%)**	**St. Dev. (%)**	**n**
Low	60-79	74.3	5.5	25
Normal	79-87	83.7	2.3	55
High	88-100	90.9	2.6	28

Table 5. Statistics for stability categories determined from the 1200 UTC NCEP/NCAR reanalysis data from an upstream point (22.5°N, 157.5°W).

Statistics for Potential Temperature				
Category	**Pot. Temp. (K)**	**Mean (K)**	**St. Dev. (m)**	**n**
Low	> -2.4	-2.0	0.3	29
Normal	-2.4 to -3.5	-2.9	0.3	55
High	< -3.5	-4.0	0.4	24

Figure Captions

Figure 1. (a) Location of hourly rainfall stations on Oahu by resolution (size of symbol), and assigned station number (#)**, (b)** Location of hourly wind stations on Oahu by source and station number.

Figure 2. **(a)** 0600 HST and (b) 1400 HST surface winds (m s^{-1}) during a strong ENE trade-wind regime averaged from May-July 2002 and May-September 2003. For the wind barbs, a half barb equals 0.5 m s^{-1}, one barb equals 1 m s^{-1}, and a flag equals 5 m s^{-1} . (c) and (d): Same as (a) and (b) but for a weak ENE trade-wind regime.

Figure 3. Time series plots of (a) the surface wind direction (degrees), (b) wind speed (m s^{-1}) during the diurnal cycle for 13 Oahu wind stations under variable wind conditions.

Figure 4. Time series of hourly rainfall frequency (%) for days with ENE trade-wind conditions from May-July 2002 and May-September 2003. Hour (HST) is on the horizontal axis, and rainfall frequency (%) is on the vertical axis.

Figure 5. Same as Figure 4 but for a strong ENE trade-wind regime.

Figure 6. Same as Figure 4 but for a weak ENE trade-wind regime.

Figure 7. Daily rainfall frequency (mm) over Oahu for 'undisturbed' days with (a) strong ENE trades, (b) normal ENE trades, (c) weak ENE trades, and (d) variable winds from May-July 2002 and May – September 2003. The contour interval for the solid lines is 2 mm and the dashed contour is 1 mm.

Figure 8. (a) Linear correlation between daily trade-wind speed (m s^{-1}) from the 1200 UTC NCEP/NCAR reanalysis data at the upstream point (22.5°N, 157.5°W) and daily trade-wind rainfall accumulation (mm) over Oahu from May-July 2002 and May-September 2003, (b) The stations with significant correlation (with 95% confidence) are plotted (large symbols).

Figure 9. Total rainfall (mm) during July-August 2005 from (a) rain guage and hydronet data (After Nguyen and Chen, 2010) , (b) WSR-88D Level III data data (Courtesy of Chuan-Chi Tu).

Figure 10. Sea-level pressure (hPa) for 'undisturbed' days with (a) high, and (b) low inversions. The contour interval is 1 hPa.

Figure 11. Daily rainfall accumulation (mm) over Oahu for (a) high, and (b) low inversion heights (m) averaged from May-July 2002 and May-September 2003. The solid contour interval is 2 mm, and the dashed contour is 1 mm. (c) and (d): Same as (a) and (b) but for daily rainfall frequencies (%). The contour interval is 20%.

Figure 12. (a) Linear correlation between daily trade-wind rainfall accumulation (mm) over Oahu and daily trade-wind inversion height (m) (12 UTC, Lihue) from May-July 2002 and May-September 2003, (b) The stations with significant correlation (with 95% confidence) are plotted (large symbols).

Figure 13. Scatter plot and correlation (R) between daily TWI height (m) determined from 1200 UTC Lihue soundings and (a) daily trade-wind speed (m s^{-1}), (b) daily RH (%) (1200 UTC at 22.5°N, 157.5°W from NCEP/NCAR reanalysis) for May-July 2002, and May-September 2003. (c) Same as (a) but between RH (%) and daily trade-wind speed.

Figure 14. Sea-level pressure (hPa) for 'undisturbed' days with (a) high and (b) low RH. The contour interval is 1 hPa.

Figure 15. Daily rainfall accumulation (mm) over Oahu for (a) high, and (b) low RH averaged from May-July 2002 and May-September 2003. The solid contour interval is 2 mm, and the dashed contour is 1 mm. (c) and (d): Same as (a) and (b) but for daily rainfall frequencies (%). The contour interval is 20%.

Figure 16. (a) Linear correlation between daily RH (%) (12 UTC from 22.5°N 157.5°W) and daily trade-wind rainfall accumulation (mm) over Oahu from May-July 2002 and May-September 2003, (b) The stations with significant correlation (with 95% confidence) are plotted (large symbols).

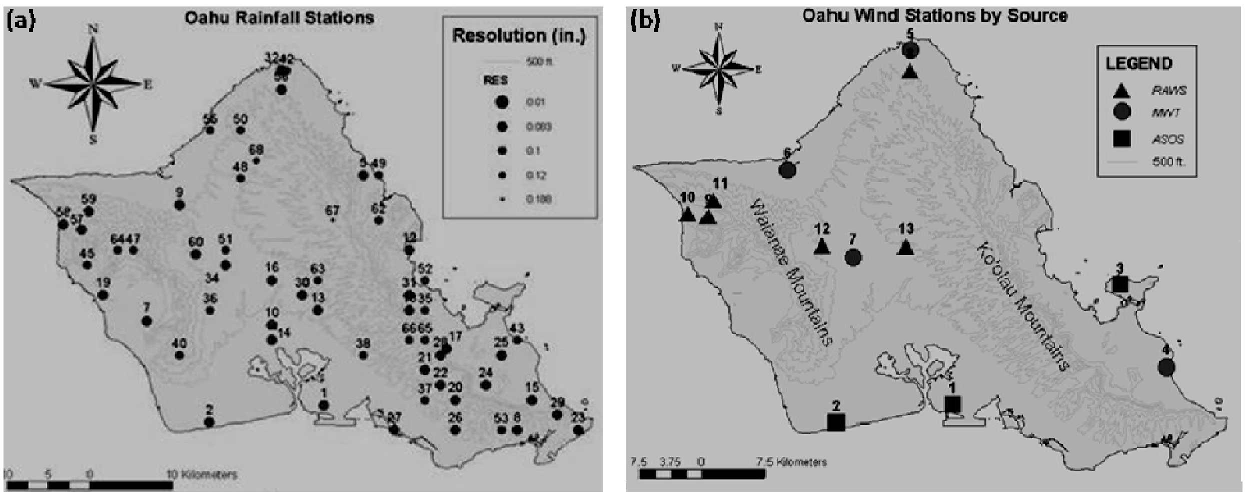

Figure 1. (a) Location of hourly rainfall stations on Oahu by resolution (size of symbol), and assigned station number (#); **(b)** Location of hourly wind stations on Oahu by source and station number.

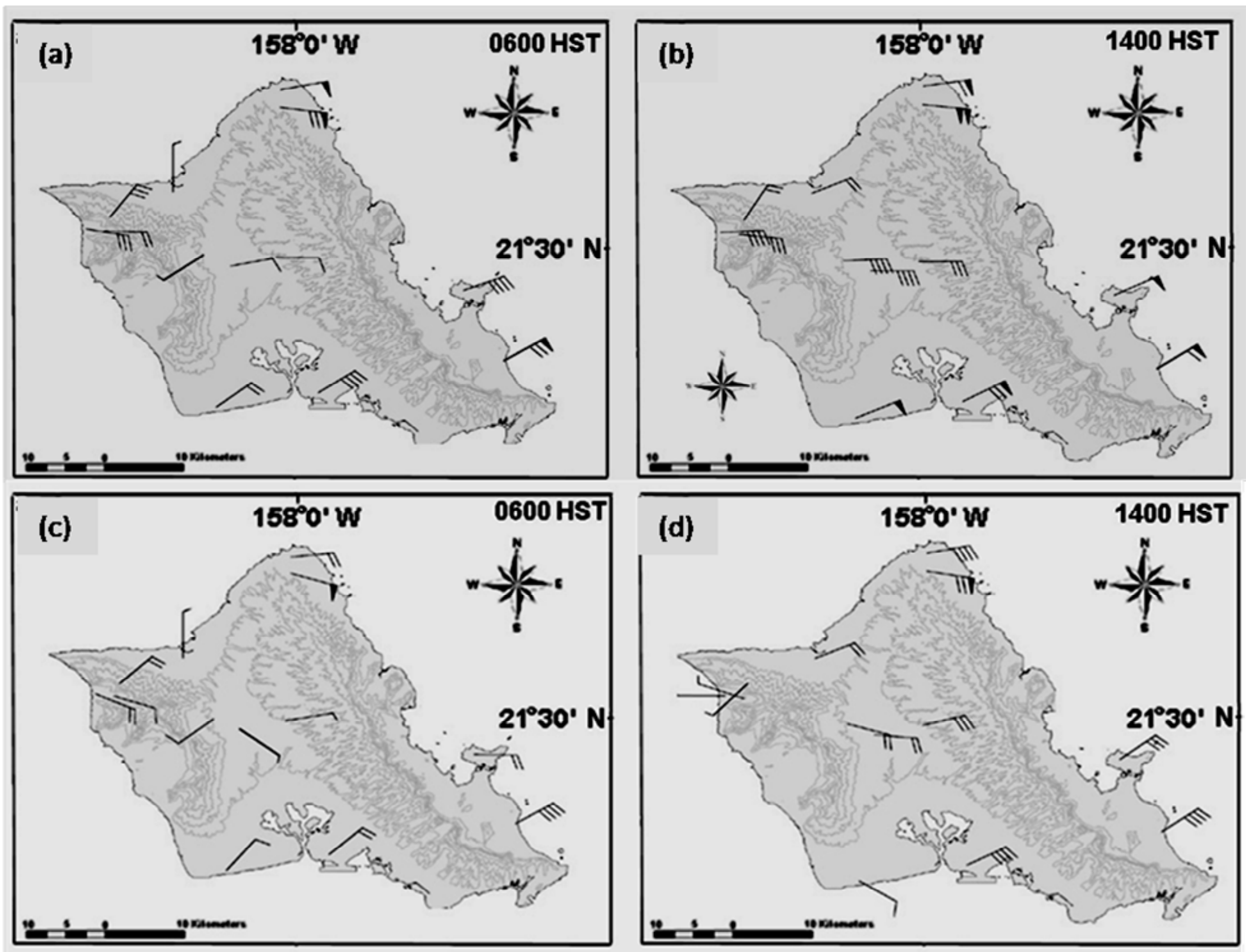

Figure 2. **(a)** 0600 HST and (b) 1400 HST surface winds (m s^{-1}) during a strong ENE trade-wind regime averaged from May-July 2002 and May-September 2003. For the wind barbs, a half barb equals 0.5 m s^{-1}, one barb equals 1 m s^{-1}, and a flag equals 5 m s^{-1} . (c) and (d): Same as (a) and (b) but for a weak ENE trade-wind regime.

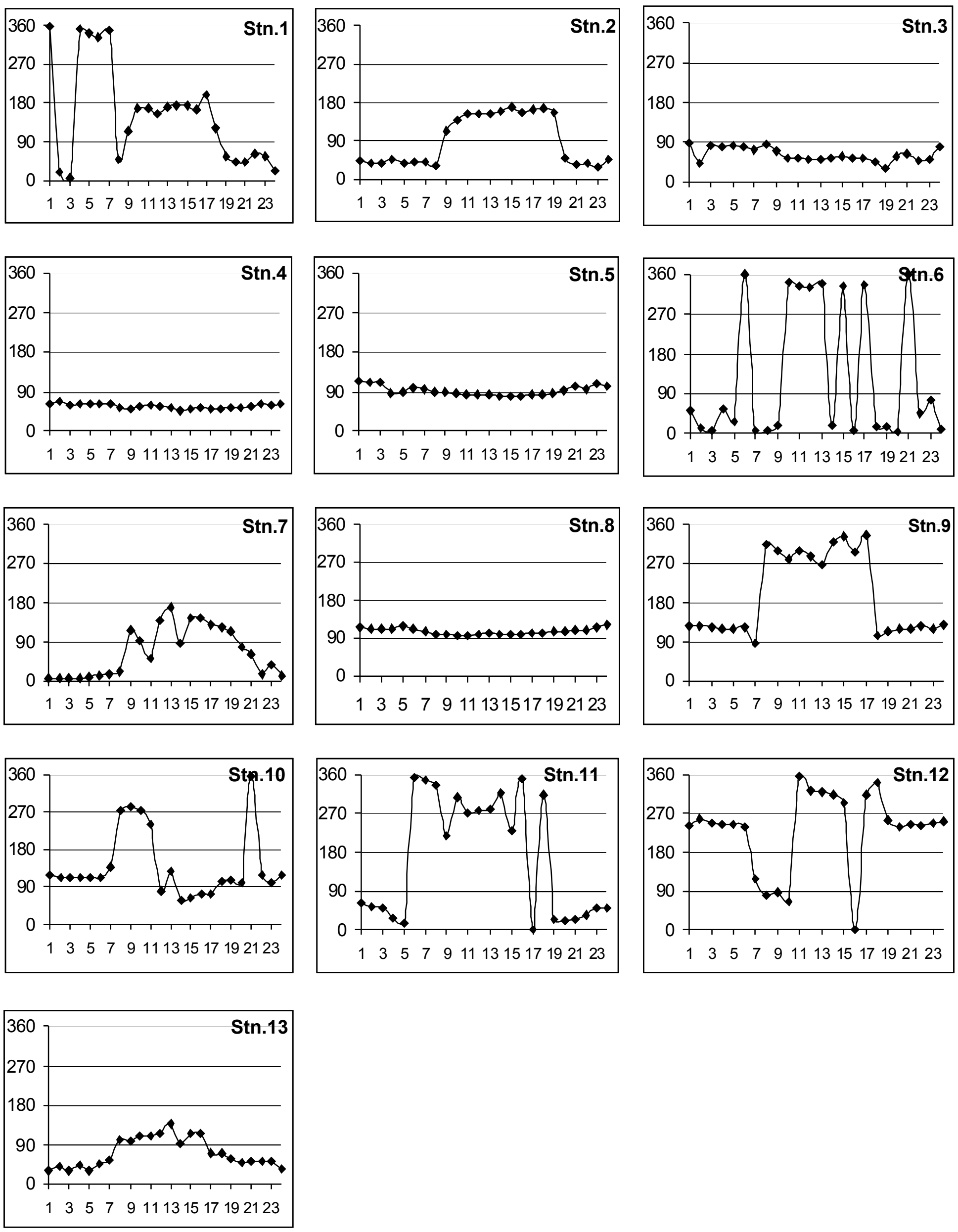

Figure 3. Time series plots of (a) the surface wind direction (degrees), (b) wind speed (m s^{-1}) during the diurnal cycle for 13 Oahu wind stations under variable wind conditions.

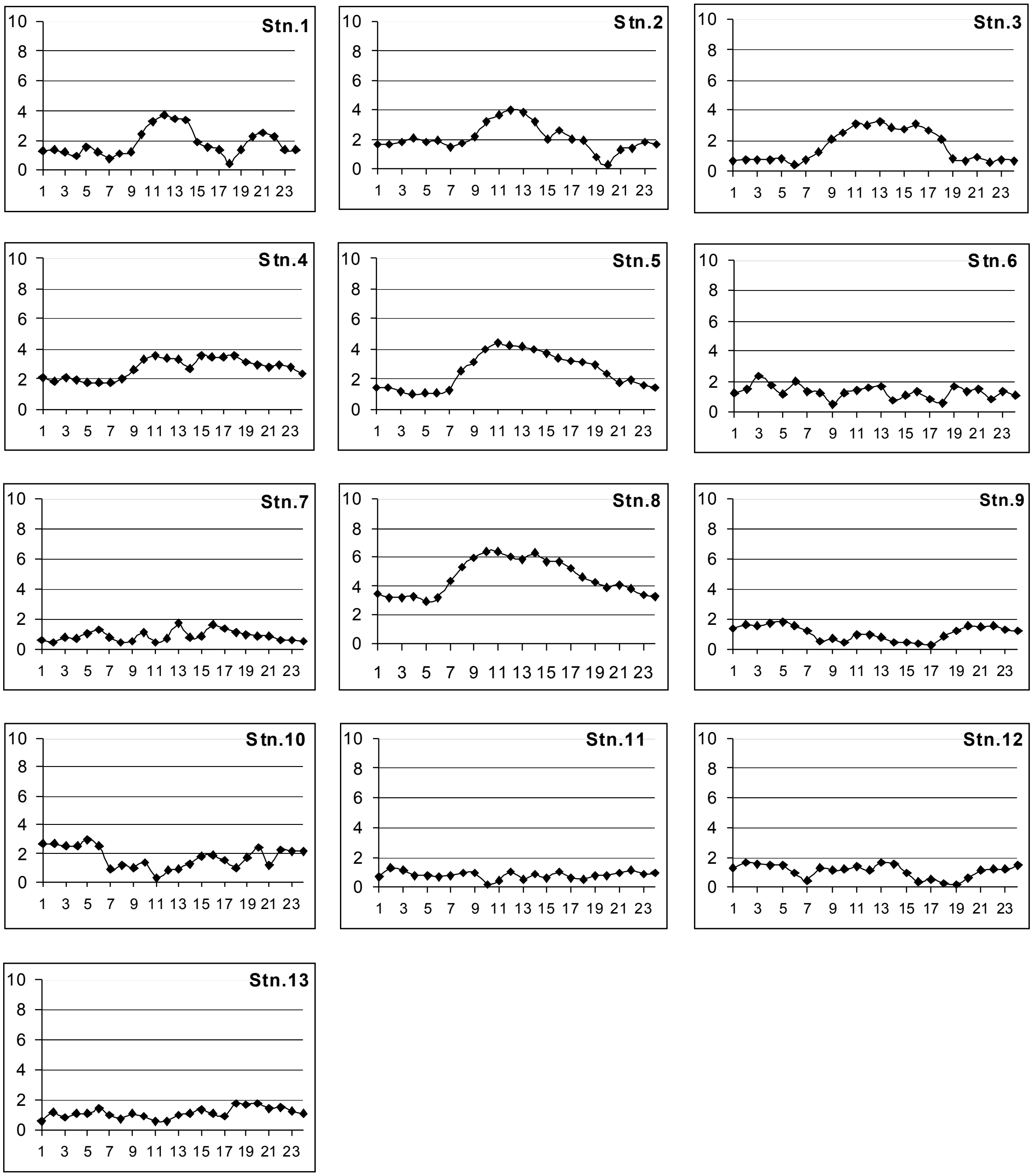
Stn.1
Stn.2
Stn.3
Stn.4
Stn.5
Stn.6
Stn.7
Stn.8
Stn.9
Stn.10
Stn.11
Stn.12
Stn.13
0 2 4 6 8 10
1 3 5 7 9 11 13 15 17 19 21 23

Figure 3b.

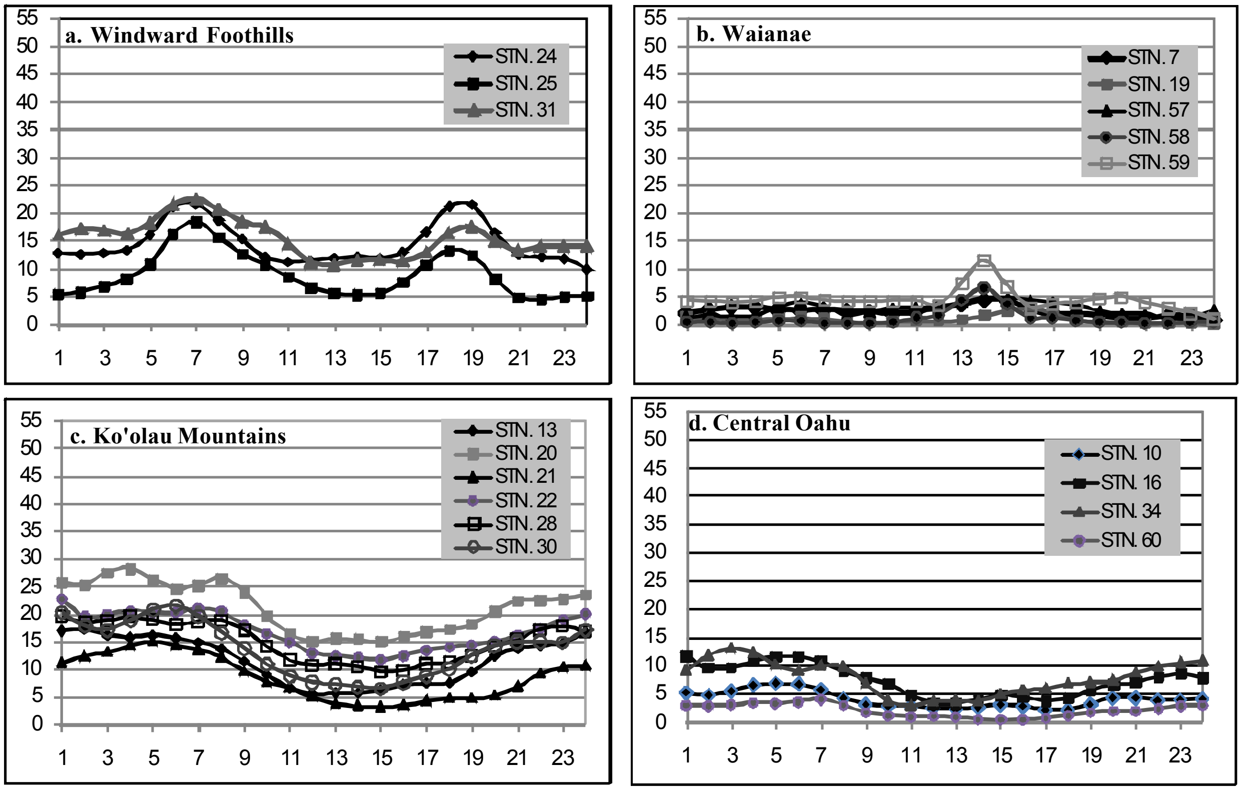

Figure 4. Time series of hourly rainfall frequency (%) for days with ENE trade-wind conditions from May-July 2002 and May-September 2003. Hour (HST) is on the horizontal axis, and rainfall frequency (%) is on the vertical axis.

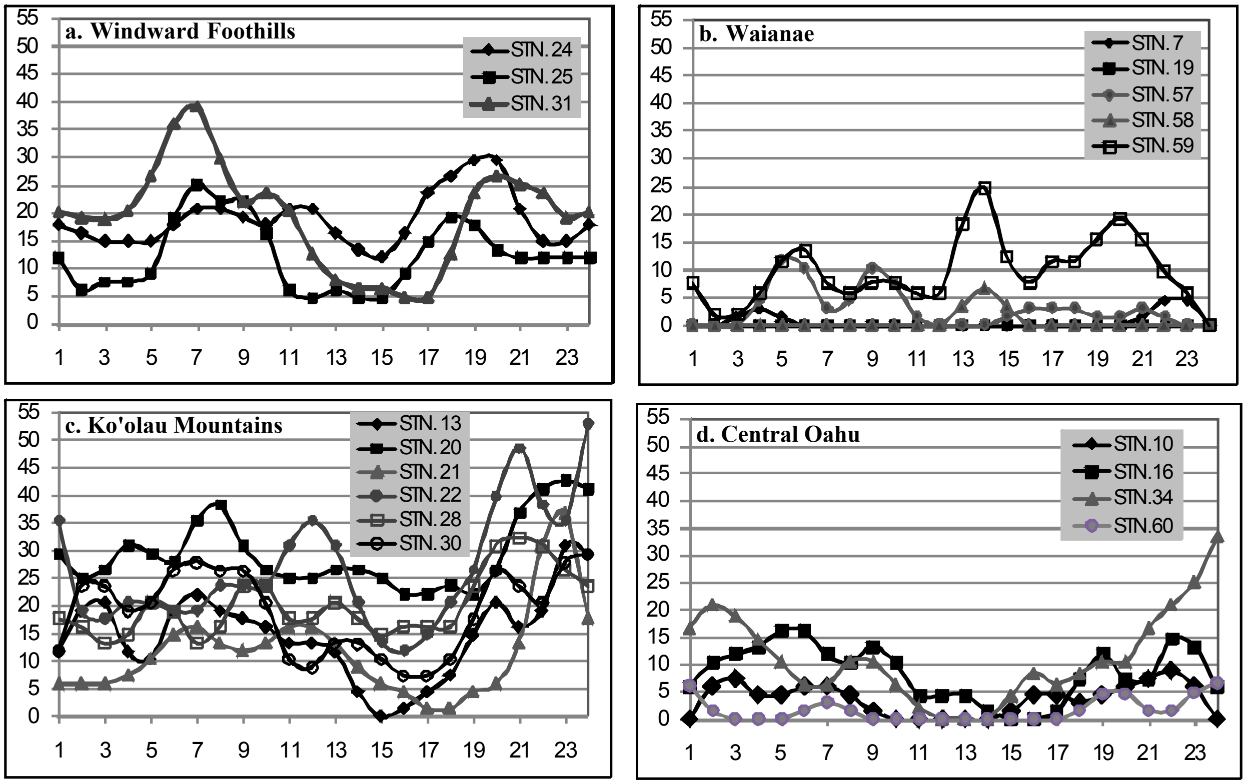

Figure 5. Same as Figure 4 but for a strong ENE trade-wind regime.

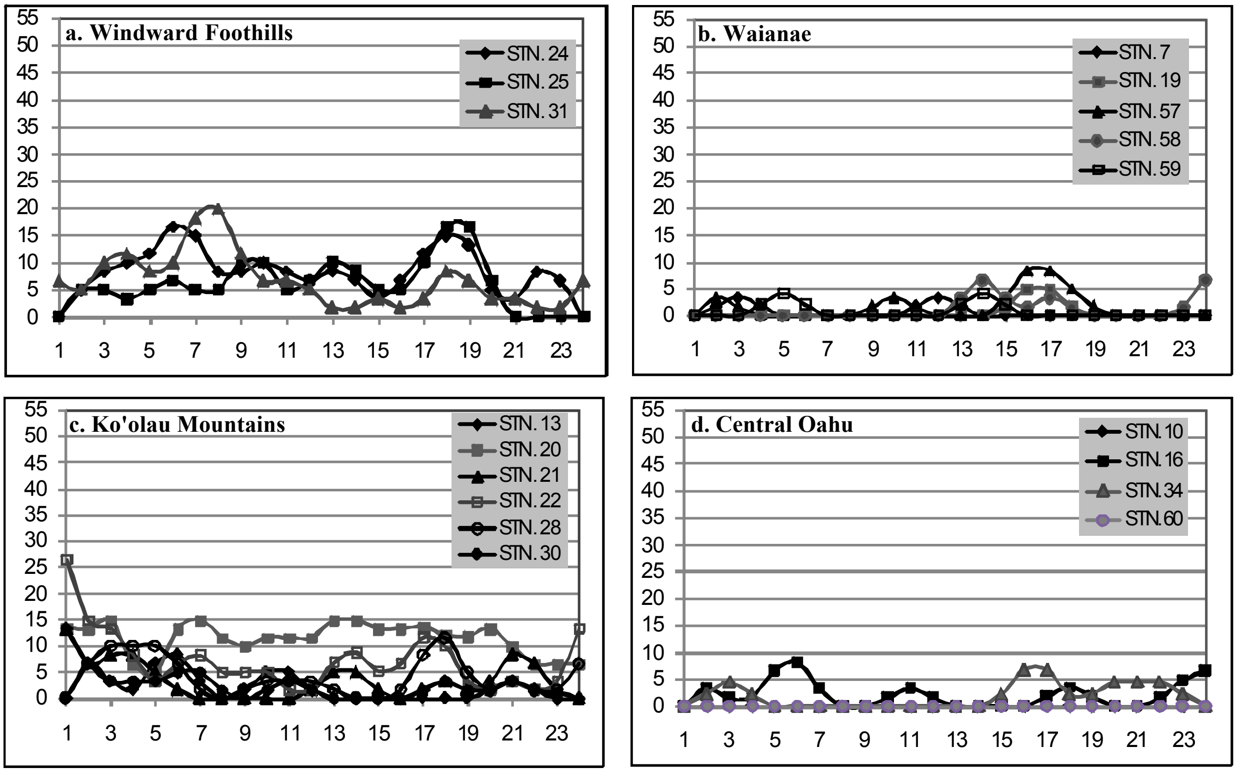

Figure 6 Same as Figure 4 but for a weak ENE trade-wind regime.

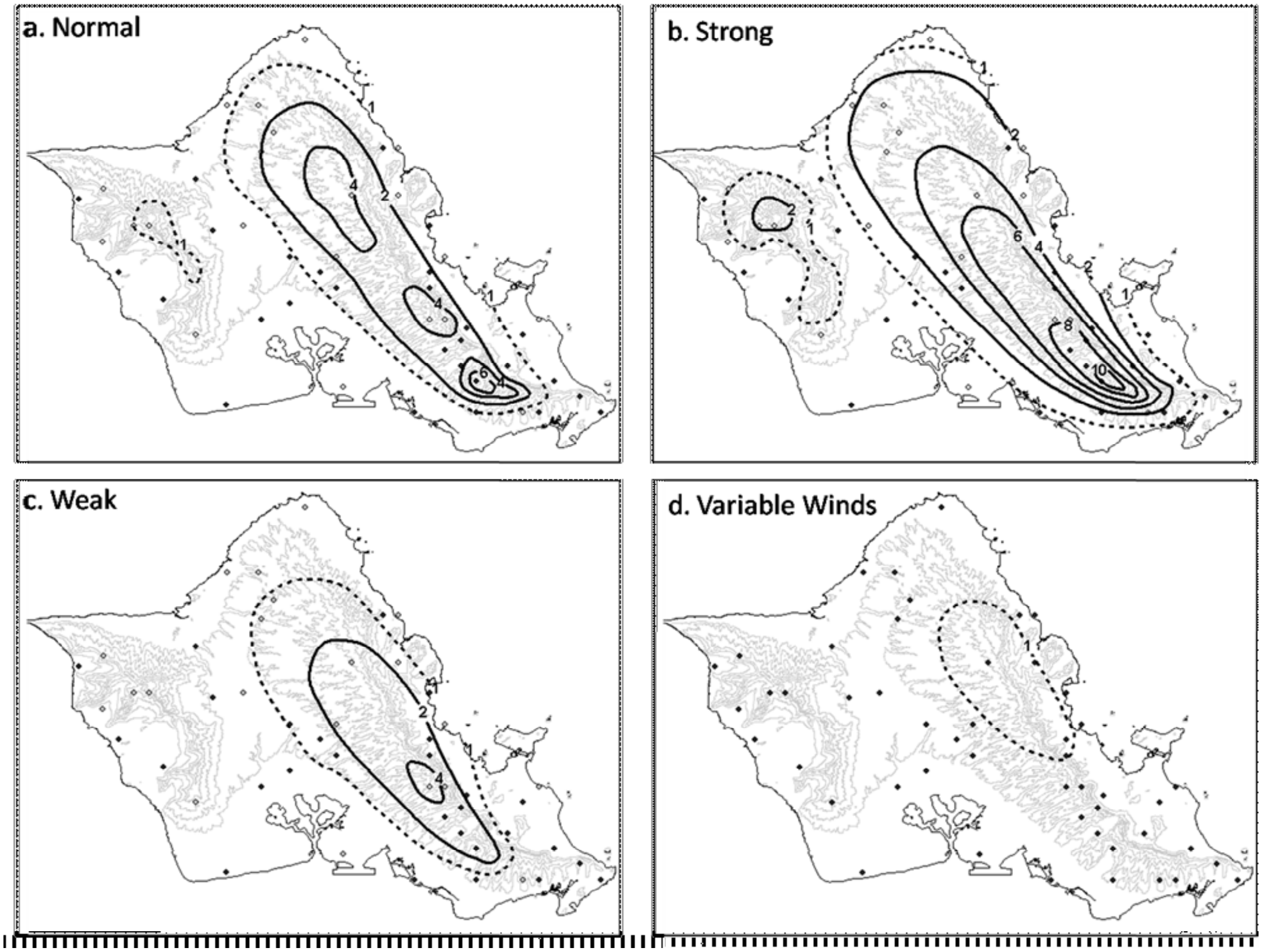

Figure 7. Daily rainfall frequency (mm) over Oahu for 'undisturbed' days with (a) strong ENE trades, (b) normal ENE trades, (c) weak ENE trades, and (d) variable winds from May-July 2002 and May – September 2003. The contour interval for the solid lines is 2 mm and the dashed contour is 1 mm.

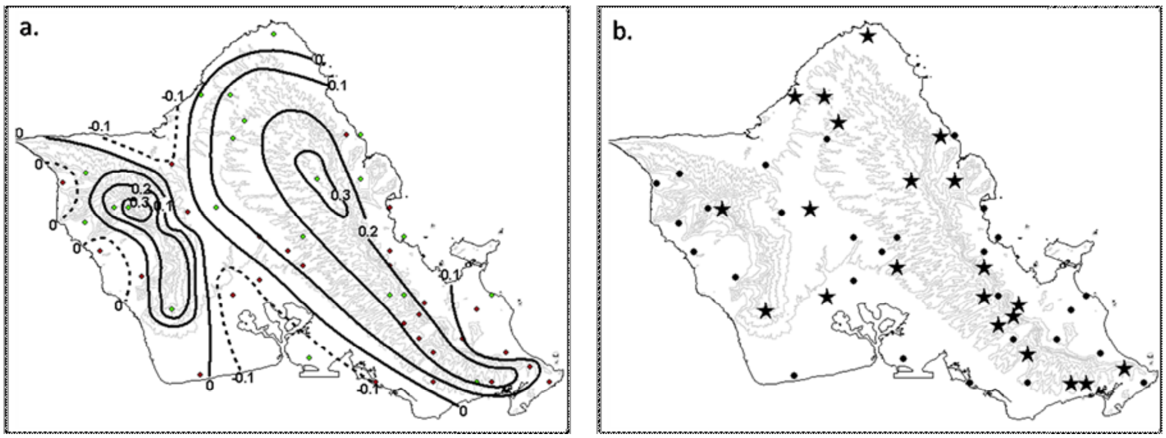

Figure 8. (a) Linear correlation between daily trade-wind speed (m s^{-1}) from the 1200 UTC NCEP/NCAR reanalysis data at the upstream point (22.5°N, 157.5°W) and daily trade-wind rainfall accumulation (mm) over Oahu from May-July 2002 and May-September 2003. (b) The stations with significant correlation (with 95% confidence) are plotted (large symbols).

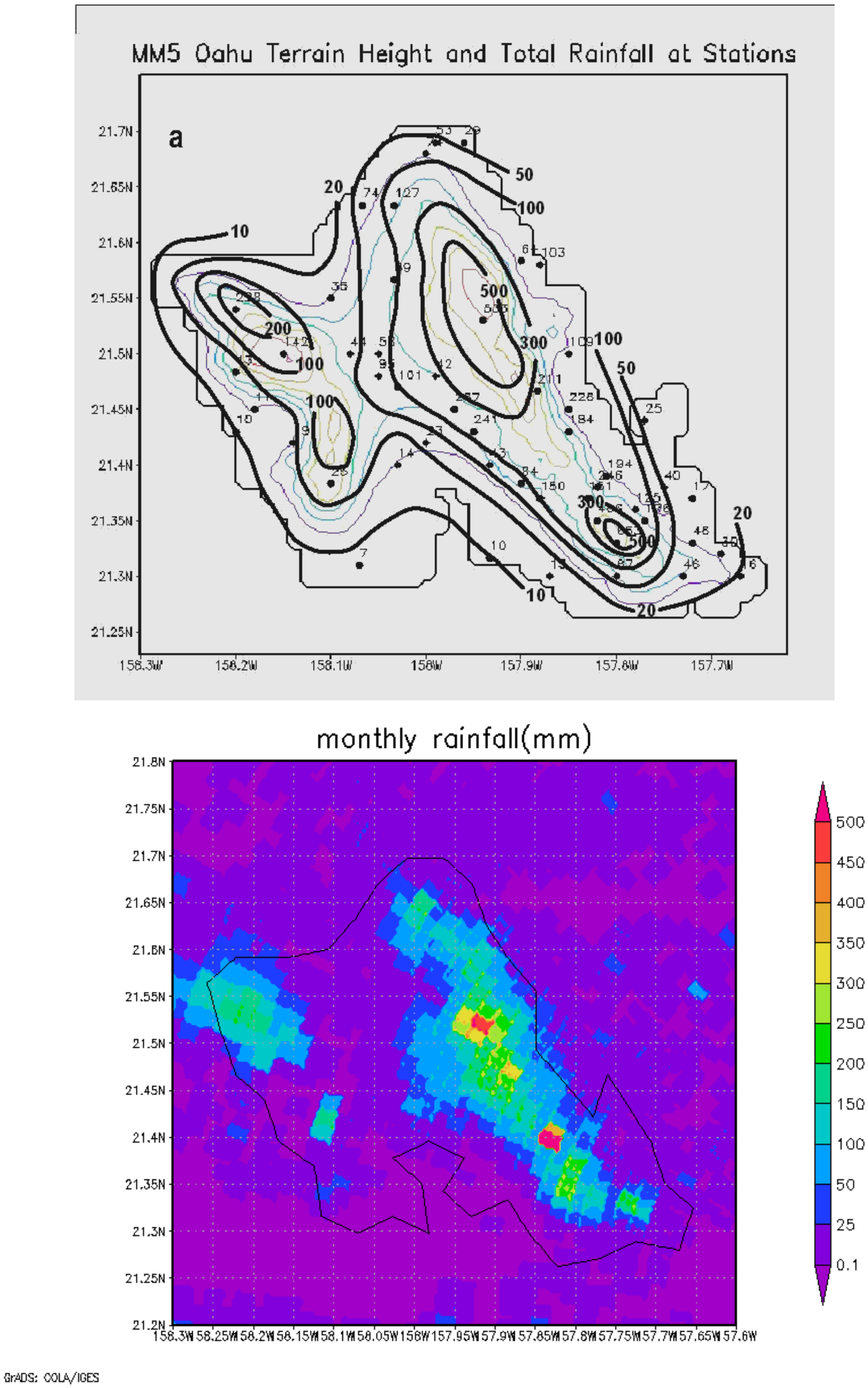

Figure 9. Total rainfall (mm) during July-August 2005 from (a) rain guages and hydronet data (after Nguyen and Chen, 2010), (b) WSR-88D Level III data (Courtesy of Chuan-Chi Tu).

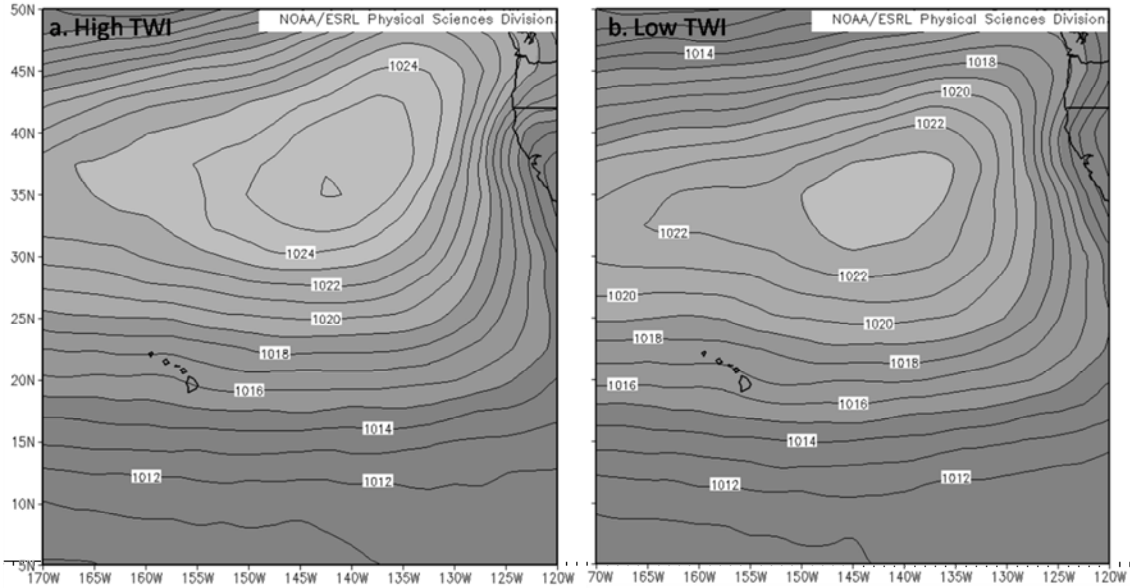

Figure 10. Sea-level pressure (hPa) for 'undisturbed' days with (a) high, and (b) low inversions. The contour interval is 1 hPa.

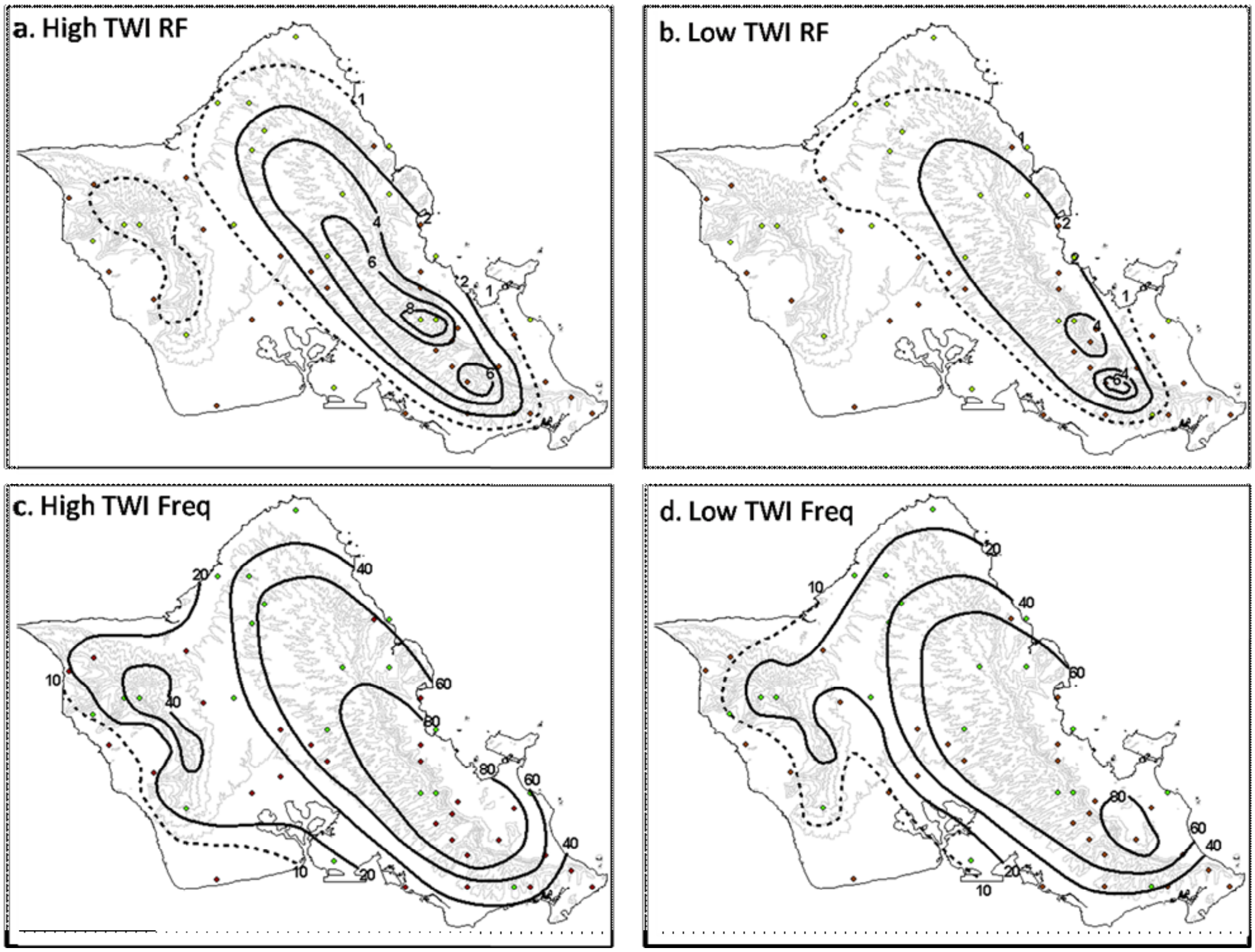

Figure 11. Daily rainfall accumulation (mm) over Oahu for (a) high, and (b) low inversion heights (m) averaged from May-July 2002 and May-September 2003. The solid contour interval is 2 mm, and the dashed contour is 1 mm. (c) and (d): Same as (a) and (b) but for daily rainfall frequencies (%). The contour interval is 20%.

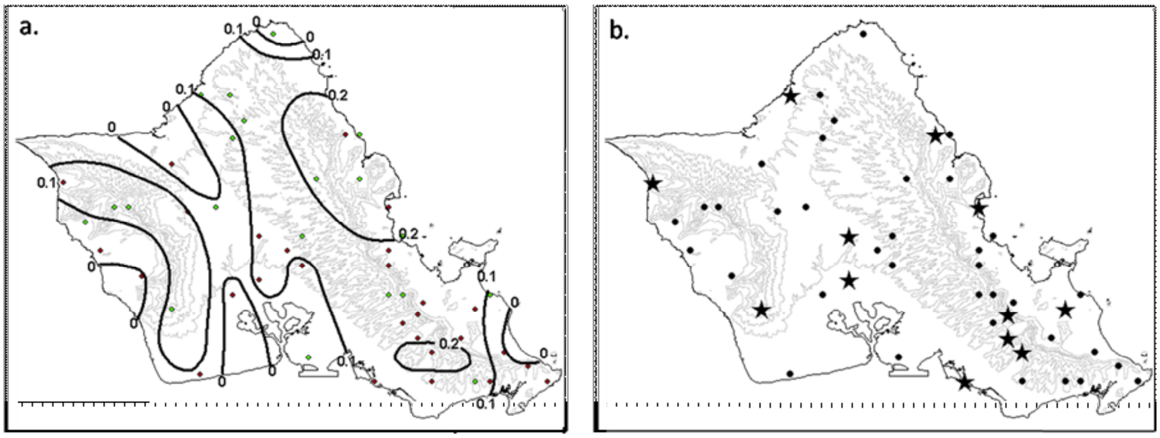

Figure 12. (a) Linear correlation between daily trade-wind rainfall accumulation (mm) over Oahu and daily trade-wind inversion height (m) (12 UTC, Lihue) from May-July 2002 and May-September 2003. (b) The stations with significant correlation (with 95% confidence) are plotted (large symbols).

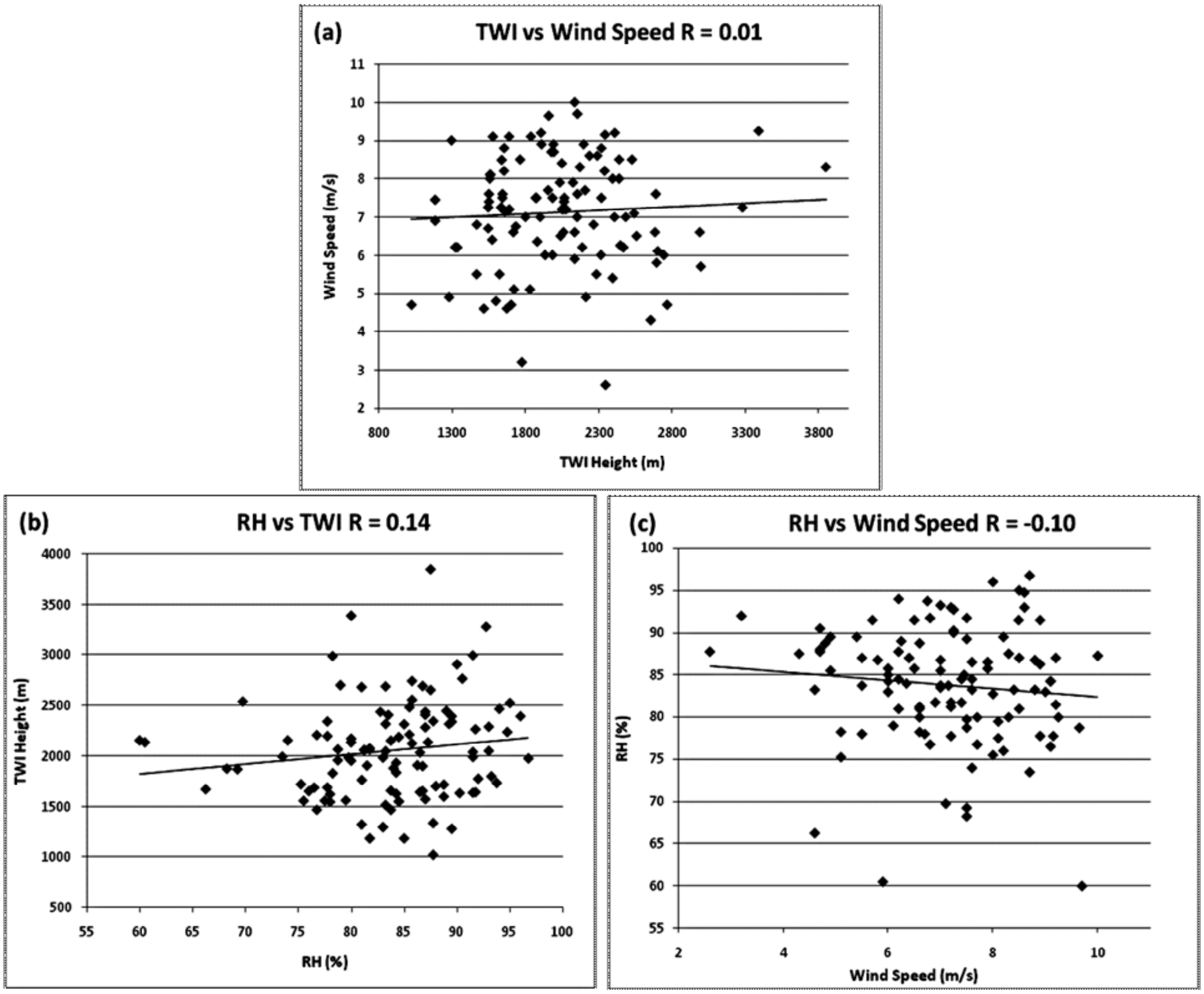

Figure 13. Scatter plot and correlation (R) between daily TWI height (m) determined from 1200 UTC Lihue soundings and (a) daily trade-wind speed (m s^{-1}), (b) daily RH (%) (1200 UTC at 22.5°N, 157.5°W from NCEP/NCAR reanalysis) for May-July 2002, and May-September 2003. (c) Same as (a) but between RH (%) and daily trade-wind speed.

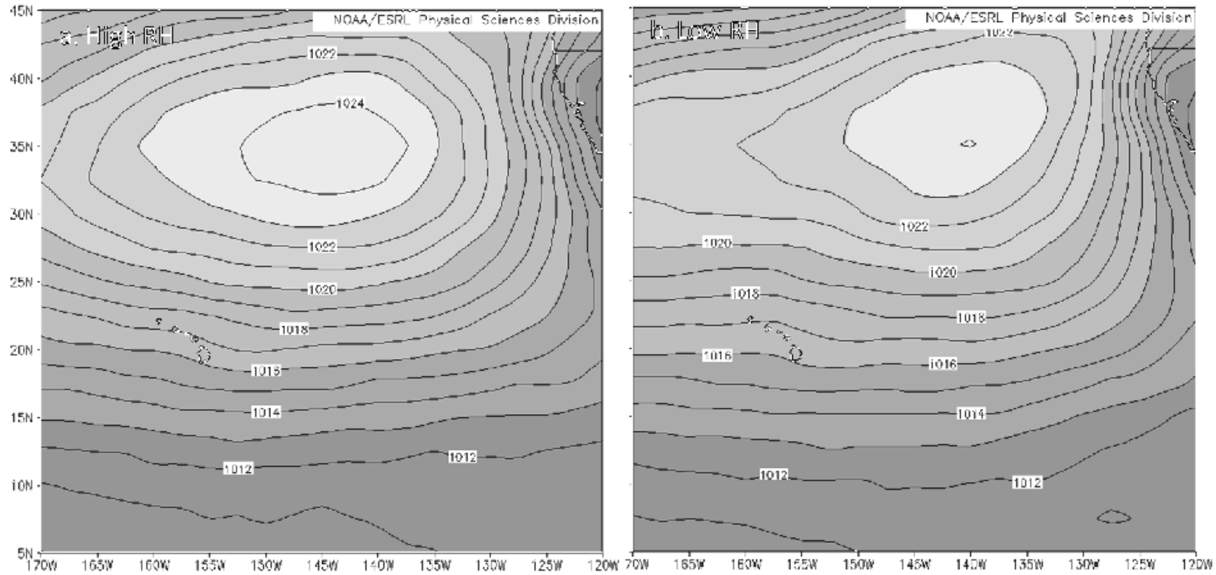

Figure 14. Sea-level pressure (hPa) for 'undisturbed' days with (a) high, and (b) low RH. The contour interval is 1 hPa.

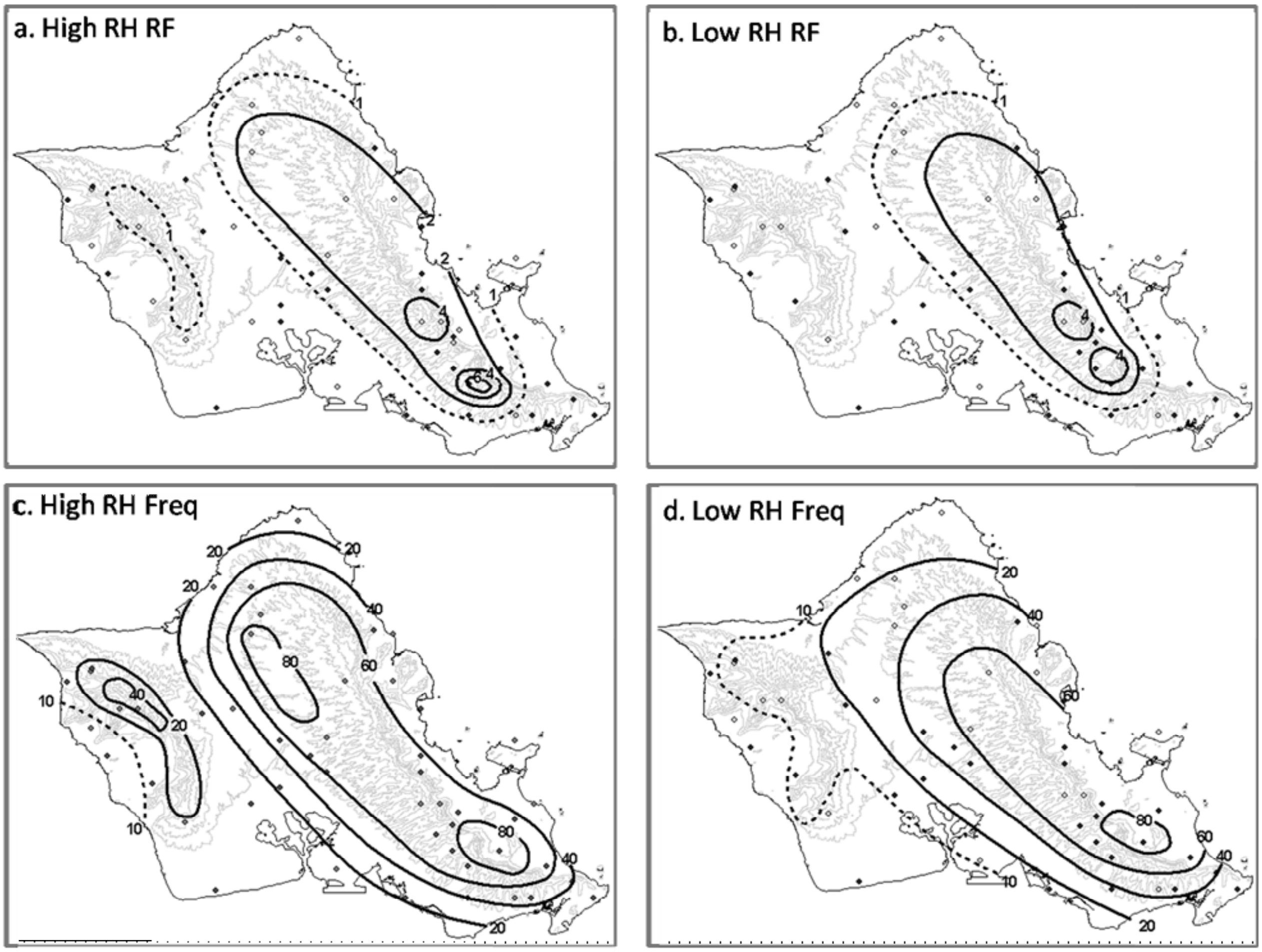

Figure 15. Daily rainfall accumulation (mm) over Oahu for (a) high, and (b) low RH averaged from May-July 2002 and May-September 2003. The solid contour interval is 2 mm, and the dashed contour is 1 mm. (c) and (d): Same as (a) and (b) but for daily rainfall frequencies (%). The contour interval is 20%.

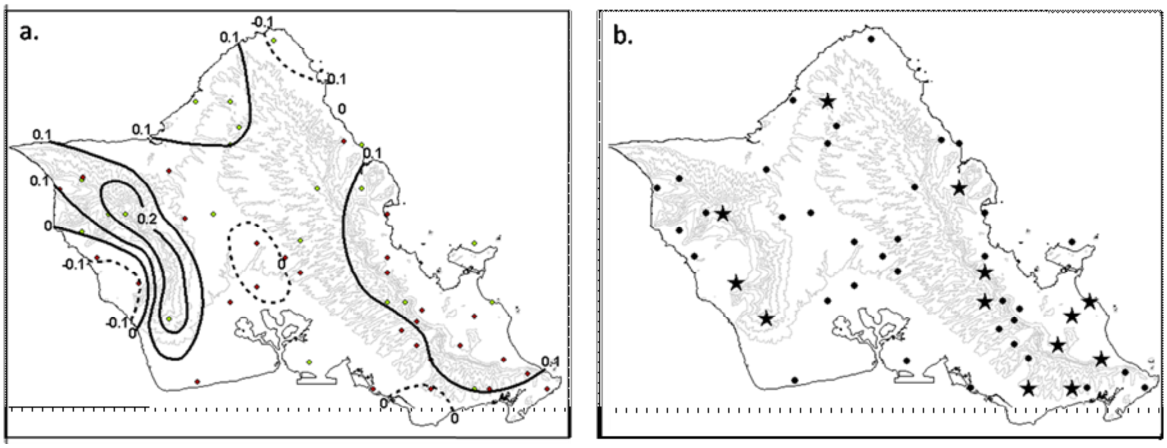

Figure 16. (a) Linear correlation between daily RH (%) (12 UTC from 22.5°N 157.5°W) and daily trade-wind rainfall accumulation (mm) over Oahu from May-July 2002 and May-September 2003. (b) The stations with significant correlation (with 95% confidence) are plotted (large symbols).